Global NEST Journal, Vol 23, No 1, pp 119-126

Removal of methylene blue dye in water by using recoverable natural zeolite/Fe_3O_4 adsorbent

Wahyuni E.T.*, Rendo D. and Suherman S.
Chemistry Department, Faculty of Mathematic and Natural Sciences, Universitas Gadjah Mada, Sekip Utara POB 21 BLS Yogyakarta, Indonesia, 55841
Received: 05/11/2019, Accepted: 18/03/2021, Available online: 09/04/2021
*to whom all correspondence should be addressed: e-mail: endang_triw@ugm.ac.id
https://doi.org/10.30955/gnj.003249

Graphical abstract

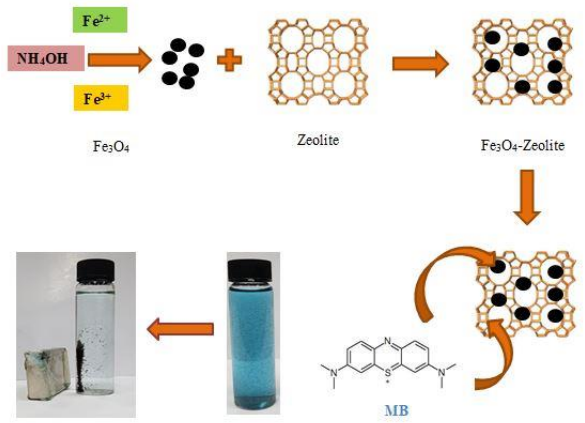

Abstract

In this paper, the low-cost and practical adsorption for removing methylene blue (MB) dye has been developed by using recoverable natural zeolite that was magnetized with Fe_3O_4. The magnetization was conducted by co-precipitation technique. The adsorbents obtained from the magnetization were characterized by XRD, FTIR, surface area analyzer and turbidity meter machines. The MB adsorption on the recoverable adsorbent was performed by batch experiment. In this study, the effect of Fe_3O_4 fraction on the recoverability and adsorption ability of the adsorbent was evaluated and the adsorption kinetic was also determined. The research results attributed that recoverable zeolite/Fe_3O_4 adsorbent has been successfully produced. It was found that the increase of Fe_3O_4 fraction in the adsorbent, has improved the recoverability, but in the same time, it caused the adsorption decreased. The fraction of Fe_3O_4 as much 33.30%w displayed compromisingly good capacity and recoverability. The maximum MB dye adsorption was reached by using 0.25 g L^{-1} of the adsorbent dose, pH 8, and in 60 min of the contact time. The adsorption kinetic well fitted with pseudo second-order with the adsorption rate of 0.0238 mg g^{-1} min^{-1}. The adsorption strongly agreed with the Langmuir isotherm with adsorption capacity of 32.258 mg g^{-1}.

Keywords: Adsorption, natural zeolite, Fe_3O_4, recoverable, adsorbent, methylene blue.

1. Introduction

Methylene blue (MB) is a cationic dye having various applications in areas, such as chemistry, biology, medical science and dyeing industries (Pathania *et al.*, 2017). Some industries widely using MB dye are the textile, plastics, rubber, leather, cosmetics and paper (Eslami *et al.*, 2017; Mouni *et al.*, 2018). These industries frequently dispose highly colored wastewater that are not only esthetically unpleasant but also hinder light penetration and may disturb the ecosystem (Meili *et al.*, 2019). Moreover, Dye wastewater contains highly toxic components that creates serious environmental impacts (Kang *et al.*, 2018). Its long-term exposure can cause vomiting, nausea, anemia and hypertension (Pathania *et al.*, 2017).

Once the dyes are exposed to water, they are difficult to remove, as they are of synthetic origin and have a very complex molecular structure, with stability designed to stand of degradation by light, chemical, biological and other factors (Ahmed *et al.*, 2017). This makes them very difficult to degrade, and consequently, wastewater treatment is one of the biggest problems we face today. Several methods have been developed to treat MB bearing effluents to bring its level down to the permissible effluent standards, including biodegradation (Eslami *et al.*, 2017), degradation by Fenton (do Cotto-Maldonado *et al.*, 2017), photocatalytic degradation (Ahmed *et al.*, 2017), and adsorption (Fan *et al.*, 2017; Kang *et al.*, 2018; Meili *et al.*, 2019; Mouni *et al.*, 2018; Saputra *et al.*, 2017; Somsesta *et al.*, 2020).

Compared with other methods, adsorption technique is currently widely applied to remove pollutants from dyeing wastewater, due to its many advantages, which include easier operation, low cost, and high efficiency (Pathania *et al.*, 2017; Fan *et al.*, 2017; Kang *et al.*, 2018; Meili *et al.*, 2019; Mouni *et al.*, 2018; Saputra *et al.*, 2017; Somsesta

et al., 2020). A large number of researchers have tried to use adsorbents such activated carbons (Pathania *et al.*, 2017), biochar (Fan *et al.*, 2017), montmorillonite/chitosan composite (Kang *et al.*, 2018), MgAL-DHL/biochar composite (Meili *et al.*, 2019), kaolin (Mouni *et al.*, 2018), activated carbon/cellulose biocomposite (Somsesta *et al.*, 2020), and natural zeolite (Saputra *et al.*, 2017) for elimination of MB dye in water.

The main problem appearing in the adsorption is the difficulty in separation of the used adsorbent from the wastewater. Recently, such problem has been solved by using separable adsorbents prepared by coating the adsorbent with magnetic material such as magnetite (Fe_3O_4). The magnetization of several adsorbents including activated carbon (Altıntıg *et al.*, 2017), clay (Ge *et al.*, 2019), and zeolites (Javanbakht *et al.*, 2017; Khodadadi *et al.*, 2017; Mohseni-Bandpi *et al.*, 2016; Yuan *et al.*, 2018) has been reported.

Of the adsorbents, zeolite have received considerable attention for contaminant removal due to its large surface area and high stability (Saputra *et al.*, 2017; Yuan *et al.*, 2018). Zeolites are hydrated aluminosilicate crystalline solids with very regular microporous structures, enclosing interconnected cavities, in which the various contaminant ions and water molecules are captured (Javanbakht *et al.*, 2017; Khodadadi *et al.*, 2017). Furthermore, when natural zeolite is used, the adsorption process becomes much cheaper (Mohseni-Bandpi *et al.*, 2016). In Indonesia, natural zeolite deposit is found abundantly and most of them is mordenite type, that has been explored as an adsorbent for removal of MB (Saputra *et al.*, 2017). Further, a magnetic Indonesian natural zeolite has also been successfully prepared to remove Pb(II) in water (Pambudi *et al.*, 2020). However, to the best of our knowledge, the research on the synthesis of magnetic Indonesian natural zeolite for MB elimination has not been forthcoming.

In the present study, we aim to modify the Indonesian natural zeolite having mordernite type by coating with magnetic Fe_3O_4 nanoparticles, and to evaluate its effectiveness in removal of MB dye from aqueous solution under different experimental conditions; including adsorbent dose, contact time, pH, and initial MB concentration. Moreover, adsorption isotherm and kinetics, were also determined.

2. Materials and method

2.1. Materials

The materials used were $FeCl_2.6H_2O$, $FeCl_3.6H_2O$, NH_4OH, HCl and NaOH from E.Merck, and were used without purification. Natural zeolite was collected from Wonosari, Yogyakarta, Indonesia that was washed with HF and EDTA before being used (Pambudi *et al.*, 2020).

2.2. Methods

2.2.1. Preparation and characterization of zeolite/Fe_3O_4 adsorbent

Zeolite-Fe_3O_4 adsorbent was performed by co-precipitation following the procedure reported previously (Mohseni-Bandpi *et al.*, 2016). For that purposes, in a 250 mL Beaker glass, 1.500 gam of the natural zeolite powder was suspended with 400 mL of 0.5 M ammonia solution. Then the suspension was heated by increasing the temperature slowly up to 70 ^oC under refluxing condition in nitrogen atmosphere with constant magnetic stirring.

Into the suspension, 100 mL solution containing 1.288 gram of $FeCl_2.6H_2O$ and 3.503 gram of $FeCl_3.6H_2O$ (giving mole ratio of Fe(II) to Fe(III) as 1:1), were added instantaneously to the resultant solution keeping at 70 ^oC for another 30 min. Then the temperature was slowly raised up to 90 ^oC for 60 min with continuous stirring. The obtained black precipitates were thoroughly rinsed with deionized water and separated by a magnet bar. Then the black solid samples were dried at 110 ^oC for about 2 h and then they were kept for characterization and adsorption. The adsorbent prepared was supposed to contain Fe_3O_4 as much as 50.00%w of the fraction. The same procedure was repeated for the processes by using natural zeolite 3.0 gram and 4.5 gram to reach Fe_3O_4 fraction as much as 33.30%w and 25.00%w respectively in the zeolite/Fe_3O_4 adsorbents. The adsorbents prepared are coded as zeolite-$Fe_3O_{4(25\%)}$, zeolite-$Fe_3O_{4(33.3\%)}$, zeolite-$Fe_3O_{4(50\%)}$, following the fraction of Fe_3O_4 in the adsorbents.

The adsorbents prepared were characterized by using 6000X Shimadzu type X-ray diffraction, Shimadzu type FTIR, surface area analyzer, and turbidity-meter. The XRD patterns of the adsorbents were recorded from 4 to 50^o of the two tetha. The FTIR spectra for adsorbents were scanned in the range of 4000–400 cm^{-1} for adsorbent samples that have been pelleted with KBr powder.

2.2.2. Adsorption experiment for MB removal by of zeolite-Fe_3O_4 adsorbent

For adsorption test, the zeolite-Fe_3O_4 adsorbents were grounded and sieved to get 250 mesh of the powder. Adsorption experiments were carried out by adding as weigh as 25 mg of a series adsorbents having different fraction of Fe_3O_4 coded as zeolite/$Fe_3O_{4(25\%)}$, zeolite/$Fe_3O_{4(33.3\%)}$, zeolite/$Fe_3O_{4(50\%)}$, as well as un-magnetic zeolite, and Fe_3O_4, to five of 250 mL beakers filled with 100 mL of 10 mg L^{-1} MB concentrations. These samples were then mounted on a magnetic plate and operated with 200 rpm with a required contact time at ambient temperature and required pH. The adsorbents were separated from the dye solutions by contacting them with magnetic rode from outside of the glass. The final MB dye concentrations in the filtrates as well as in the initial solution were determined by UV-Visible spectrophotometer. The concentrations of the MB adsorbed were obtained from the difference of the initial and final dye concentrations in solution.

The same procedure was applied for adsorption with various condition processes that were 5, 15, 30, 45, 60, 90, 120, 180 min of the contact time, 5, 10, 15, 20, 25, 30, 40 mg of the adsorbent weigh, 1, 3, 5, 7, 9, 11, 13 of the solution pH, and 5, 10, 20, 30, 40, 50 mg L^{-1} of the initial MB concentrations. When one variable was varied, the others were kept constant. The percentage adsorption of MB was calculated according to:

$$\text{Removal MB (\%)} = (W_0 - W_e)/W_0 \times 100\%$$

The adsorption capacity of the MB dye was calculated as Eq. 1 below:

$$W = (C_0 - C_e)V/m \quad (1)$$

where W, the amount of MB adsorbed per unit mass of the adsorbent (mg g^{-1}); W_0, the initial mass of MB; W_e, the final mass of MB after adsorption; C_0, initial concentration of MB in the aqueous solution (mg L^{-1}); C_e is the final equilibrium concentration of test solution (mg L^{-1}); m, mass of the adsorbent (g); and V, volume of sample (L).

3. Results and discussion

3.1. Characters of zeolite-Fe_3O_4 adsorbent

The reactions occurred during the preparation were presented as Eq. 2 (Mohseni-Bandpi *et al.*, 2016).

$$\text{Zeolite}_{(s)} + 2Fe^{3+}_{(aq)} + Fe^{2+}_{(aq)} + 8\ OH^-_{(aq)} \rightarrow \text{Zeolit/}Fe_3O_{4(s)} + 4H_2O_{(aq)} \quad (2)$$

The color of the natural zeolite was observed to change from light green into blackish after being covered by Fe_3O_4. The color of the magnetize zeolite (zeolite/Fe_3O_4) was darker as the fraction of Fe_3O_4 increased, follows the color of Fe_3O_4. It is inferred that the solid magnetite (Fe_3O_4) may be formed on the surface of zeolite structure.

3.1.1. XRD data

The XRD patterns of the un-magnetized natural zeolite, the synthesized Fe_3O_4, and the magnetized natural zeolite (zeolite/Fe_3O_4) are displayed as Figure 1. It is seen in the figure that the natural zeolite has several characteristic peaks, that are 2θ=5.42°, 9.62°, 13.18°, 19.40°, 22.05°, 25.43°, 26.06°, 27.41°, 30.65° and 35.07°. These peaks match with JCPDS No. 5-0490 of mordernite zeolite type, that is in a good agreement with the data reported previously (Pambudi *et al.*, 2020). In the XRD pattern of Fe_3O_4 several peaks of 2θ = 30.09°, 35.36°, and 43.21°are observed, that are associated to (220), (311), (400), (422), (511) and (440) phase, respectively (Mohseni-Bandpi *et al.*, 2016).

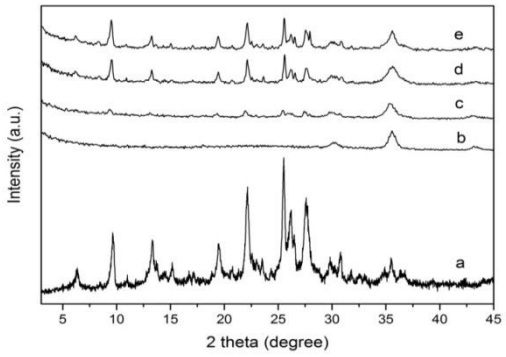

Figure 1. The XRD patterns of (a) natural zeolite, (b) Fe_3O_4, (c) zeolite/$Fe_3O_{4(50\%)}$, (d) zeolite/$Fe_3O_{4(33.3\%)}$, and (e) zeolite/$Fe_3O_{4\ (25\%)}$

The XRD patterns of the magnetized adsorbents (zeolite/Fe_3O_4) exhibit characteristic peaks of the natural zeolite along with the peaks of Fe_3O_4. Further, it can also be seen that the intensities of the zeolite patterns are reduced and become wider as the Fe_3O_4 fraction increases or the fraction of the zeolite decreases. It is reasonable since the intensity is proportional to the amount of the crystal. Other study has also found the same data (Mohseni-Bandpi *et al.*, 2016; Pambudi *et al.*, 2020). This data suggested that Fe_3O_4 has coated the zeolite structure as desired.

3.1.2. FTIR data

In the FTIR spectra of Fe_3O_4, peak bands around 3428 and 571 cm^{-1} are observed. The band of 571 cm^{-1} is related to Fe–O stretching band that is the characteristic peak of Fe_3O_4. The peak at 3440 cm^{-1} may be assigned to hydroxyl group from water adsorbed on its surface (Mohseni-Bandpi *et al.*, 2016). The FTIR spectra for natural zeolite exhibit some bands around 3627, 3448, 1636, 1049, and 463 cm^{-1}. The bands located around 3627 and 3448 cm^{-1} are typically attributed to the -OH group. The band at 1636 cm^{-1} is due to bending vibration of OH from adsorbed water. Band at 1049 cm^{-1} is associated for Al-O-Si chain of zeolite group. Bands around 606 and 471 cm^{-1} are assigned to the Si-O-Si stretching as well as bending vibrations of condensed silica (Mohseni-Bandpi *et al.*, 2016). Compared to the FTIR spectra of natural zeolite, reducing percent transmittance (%T) values of the zeolite peaks from zeolite/Fe_3O_4 samples were observed but the wavenumbers remain unchanged. Moreover, the trans-mittance reduces as the fraction of Fe_3O_4 in the adsorbent increases. This provides evidence that the zeolite structure remains unchanged after the coating with Fe_3O_4 (Pambudi *et al.*, 2020). Furthermore, new adsorption peaks at 3155 cm^{-1} and 1409 cm^{-1} were observed corresponding to Fe-O stretches of Fe_3O_4, this indicates the successful coating of Fe_3O_4 particles on the zeolite surface (Mohseni-Bandpi *et al.*, 2016).

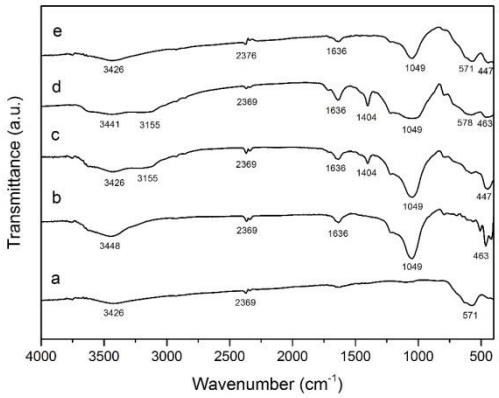

Figure 2. FTIR spectra of : (a) Fe_3O_4, (b) zeolite, (c) zeolite/$Fe_3O_{4(25\%)}$, (d) zeolite/$Fe_3O_{4(33.3\%)}$, and (e) and (c) zeolite/$Fe_3O_{4(50\%)}$

3.1.3. Surface characters

The characters associated with the surface are also measured as exhibited in Table 1. It is shown that magnetization to the zeolites can increase their surface area, enlarge their pore size, and add the pore volumes. The increase of the surface characters is found to be correlated directly with the increase of the fraction of F_3O_4

in the adsorbents. The increase of the zeolite surface area indicates that Fe_3O_4 particles could extent the zeolite surface. Enlargement of the zeolite pores may be not caused by opening the pores, but it is more possible due to the formation of new larger pores by Fe_3O_4 particles on the zeolite surface. An increase in the total pore volume implies that covering Fe_3O_4 on the zeolite structure can create new pores, and the pore size are larger as probed by the enlargement of the pore size of zeolite/Fe_3O_4 adsorbents (Mohseni-Bandpi *et al.*, 2016).

Table 1. Surface characters of the adsorbents

Adsorbent	S_{BET} (m^2g^{-1})	$V_{pore\ total}$ (mL g^{-1})	R_{pore} (Å)
Zeolite	55.64	0.0625	21.68
Zeolite/$Fe_3O_{4(25\%)}$	124.5	0.2914	21.12
Zeolite/$Fe_3O_{4(33.3\%)}$	170.4	0.3246	23.76
Zeolite/$Fe_3O_{4(50\%)}$	194.2	0.3534	32.08

3.1.4. SEM data

SEM images were made to investigate the surface morphology of the magnetized zeolites. The images of the natural zeolite, Fe_3O_4, and zeolite/Fe_3O_4 are illustrated in Figure 3.

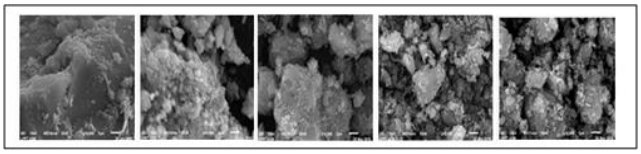

Figure 3. SEM images of: (a) natural zeolite, (b), Fe_3O_4, (c) zeolite/$Fe_3O_{4(25\%)}$, (d) zeolite/$Fe_3O_{4(33.3\%)}$, (e) zeolite/$Fe_3O_{4(50\%)}$

The SEM images of zeolite/Fe_3O_4 show that the zeolite was covered by smaller particle of Fe_3O_4. Increasing fraction of Fe_3O_4 shows more particles covering the big phase of the zeolite. The similar finding was also reported previously (Yuan *et al.*, 2018). This provides evidence that Fe_3O_4 has layered the zeolite, and this well fits with the XRD and FTIR data.

3.1.5. Recoverability of the adsorbents

The recoverability of the magnetized adsorbents (zeolite/Fe_3O_4) were evaluated by observing their physical appearance, and the results are displayed as Figure.4. The figure attributes that the increase of Fe_3O_4 fraction in the adsorbent gives clearer solution implying the better separation. It is clearly proven that zeolite/Fe_3O_4 prepared are magnetic and recoverable adsorbents (Yuan *et al.*, 2018).

The recoverability can be also represented by turbidity values, as seen in Figure 5. The figure exhibits a decline in the turbidity as the Fe_3O_4 fraction in the adsorbent raises. The smaller turbidity shows that the adsorbent has better recoverability. It is clear that recoverability is proportional to the Fe_3O_4 fraction, that is reasonable since the magnetic property is possessed by Fe_3O_4. Further, this turbidity data is also consistence with the data of separation appearance (Pambudi *et al.*, 2020).

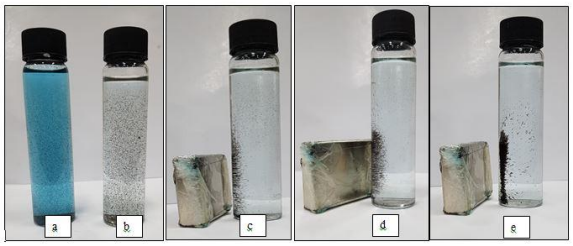

Figure 4. (a) A mixture of adsorbent and MB before adsorption, (b) A mixture of adsorbent and MB after adsorption, (c) zeolite/$Fe_3O_{4(25\%)}$, (d) zeolite/$Fe_3O_{4(33.3\%)}$, and (e) zeolite/$Fe_3O_{4(55\%)}$

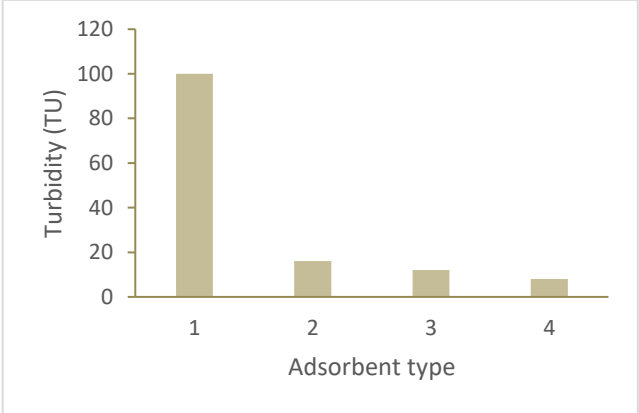

Figure 5. The influence of Fe_3O_4 fraction in the adsorbents on the turbidity of the solution that has been separated from the adsorbent. (1) Zeolite, (2) zeolite/$Fe_3O_{4(25\%)}$, (3) zeolite/$Fe_3O_{4(33.3\%)}$, and (4) zeolite/$Fe_3O_{4(50\%)}$

3.2. Adsorption activity of zeolite/Fe_3O_4 adsorbent

The adsorption effectiveness of MB dye by un-magnetized and magnetized zeolites (zeolite/Fe_3O_4) were exhibited in Figure 6.

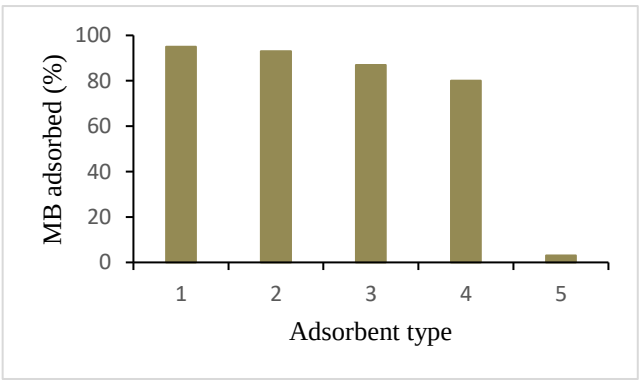

Figure 6. MB adsorption efficiency on (1) zeolite, (2) zeolite/$Fe_3O_{4(25\%)}$, (3) zeolite/$Fe_3O_{4(33\%)}$, (4) zeolite/$Fe_3O_{4(50\%)}$, and (5) Fe_3O_4

From the figure, it is observable that magnetization of the natural zeolite (zeolite/Fe_3O_4) leads to the adsorption slightly decreased, although the surface area of all magnetized zeolite samples or zelite-Fe_3O_4 adsorbents were measured to be larger than the un-magnetized one. It is implied that Fe_3O_4 covering the zeolite surface reduced the adsorption active surface, and the reducing active surface is proportional to the Fe_3O_4 fraction. A decrease in the adsorption may be caused by blocking the zeolite pores

by Fe_3O_4. It is also shown that Fe_3O_4 was able to adsorb MB in very low capability. Some studies found that magnetization on the adsorbent slightly decrease the adsorption capacity, but is not considerable (Yuan *et al.*, 2018). The high adsorption as well as good separation is shown by the adsorbent of zeolite/$Fe_3O_{4(33.3\%)}$, where the adsorbent is covered by medium amount of Fe_3O_4 that still provided adsorbent active surface as well as magnetic property.

3.2.1. Influence of adsorbent dose

Since adsorbent dose is important factor determining the adsorption effectiveness, in this paper the influence of the adsorbent dose was examined, and the data was displayed as Figure 7. In the figure, improvement of the MB adsorption is attributed when the adsorbent dose was increased, but the further increase of the adsorbent dose beyond 25 mg in 100 mL no significant changes in the MB removal efficiency were observed. Increasing adsorbent dose provides more active surface for MB dye, consequently better adsorption takes place. When the adsorbent dose was larger than 25 mg in 100 mL, the suspension became denser that could inhibit the interaction between MB and the adsorbent active surface. Accordingly no adsorption improvement is demonstrated.

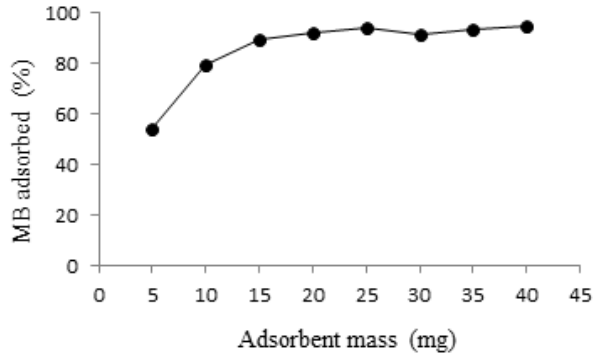

Figure 7. The influence of the adsorbent dose on the MB adsorption

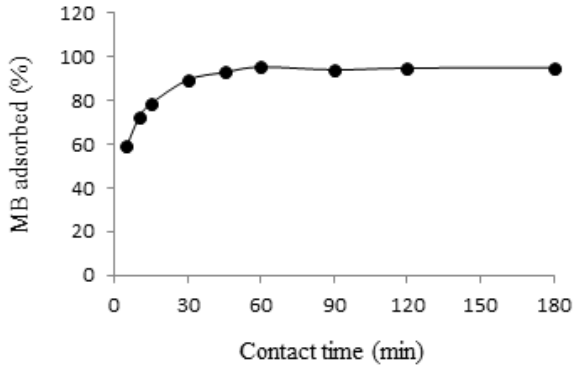

Figure 8. The influence of the contact time on the effectiveness of MB adsorption

3.2.2. Influence of contact time

The influence of the contact time on the adsorption results is shown by Figure 8. The trend of the graph shows that as the contact time extended up to 60 min, the percentage removal also increases, until it reaches a maximum level. The further of the extension longer than 60 min in contact time does not change the percentage removal. Initially all the adsorbent sites are vacant that promote very fast adsorption. The contact time longer than 60 min, the surface of the adsorbent may be mostly occupied or saturated with MB molecules, that no more sites for MB adsorption. This trend indicates the possible monolayer formation of MB on the adsorbent surface (Pathania *et al.*, 2017).

3.2.3. Influence of solution pH

pH is a key factor during the adsorption process and control the surface of the adsorbent and the speciation of MB in the solution. The results of the adsorption with the alteration pH are displayed in Figure 9. A slight decrease of the adsorption with increasing pH is demonstrated in the figure. MB is a basic dye that gives positively charged ions when it dissolved in water, meanwhile zeolite surface has negative charges. Thus, in acidic medium, the positively charged surface of the adsorbent may be occurred that tends to oppose the adsorption of the cationic dye. When pH of the dye solution is further increased the adsorbent surface acquires a negative charge, there by resulting in an increased adsorption of MB due to an increase in the electrostatic attraction between positively charged dye and negatively charged adsorbent. Hence pH 8 is suggested to be the optimum value, that was same finding as found by Pathania *et al.* (2017).

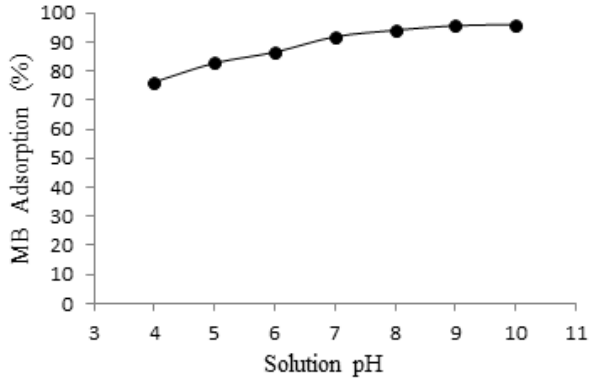

Figure 9. The influence of the solution pH on the effectiveness of the MB adsorption

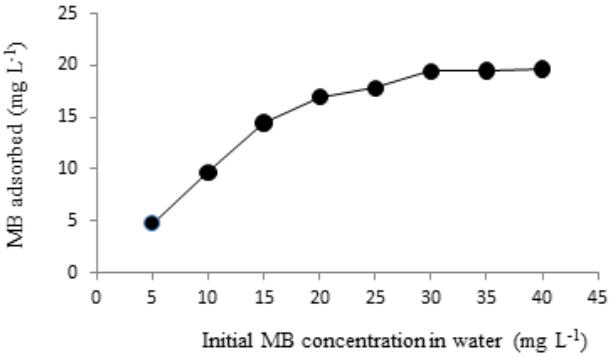

Figure 10. The influence of the initial MB concentration on the adsorption

3.2.4. Influence of the initial MB concentration

As seen in Figure 10, that increasing the initial MB concentration improves the MB adsorption, but the adsorption is not depend on the concentration for the

initial concentration higher than 25 mg L^{-1}. This is due to the fact that with increasing dye concentration, the driving force for mass transfer also enhances. Above optimal MB concentration, most adsorption active sites may be occupied by MB, leading to lack of the active sites for the adsorption (Mohseni-Bandpi *et al.*, 2016).

From the optimization results, it is found the that the adsorbent has saturated after 60 min for taking 25 mg L^{-1} of the MB initial concentration. In order to be able to reuse, the saturated adsorbent has to be regenerated. The regeneration can be performed by desorption using corresponding organic solvent or.

3.2.5. Adsorption Kinetic

The adsorption kinetic was examined for a better understanding of MB adsorption on zeolite/Fe_3O_4 adsorbent and providing a predictive model that allows the estimation of the amount of ions adsorbed during the process. The data was plotted for equations both for pseudo-first order and pseudo second-order following Eq. 3 and Eq. 4 respectively:

$$\ln(q_e - q_t) = \ln q_t - kt \quad (3)$$

$$\frac{t}{q_t} = \frac{1}{kq_e^2} + \frac{t}{q_e} \quad (4)$$

The results were displayed in Figure 11 and Table 2, where the MB adsorption well fits with the pseudo second-order, as indicated by correlation coefficient (R^2) as much as 0.9998 that is higher than that of pseudo first-order, 0.9071. This confirmed that the rate limiting step is chemisorption, involving valence forces through sharing or exchange of electron (Pathania *et al.*, 2017).

Table 2. The kinetic parameters of the adsorption

Reaction kinetic	Parameter	Zeolite/Fe_3O_4 adsorbent
Pseudo first-order	R^2	0.9071
	q_e (mg g^{-1})	3.5537
	k_1 (min^{-1})	0.0286
Pseudo second-order	R^2	0.9998
	q_e (mg g^{-1})	15.5038
	k_2 (g mg^{-1} min^{-1})	0.0238

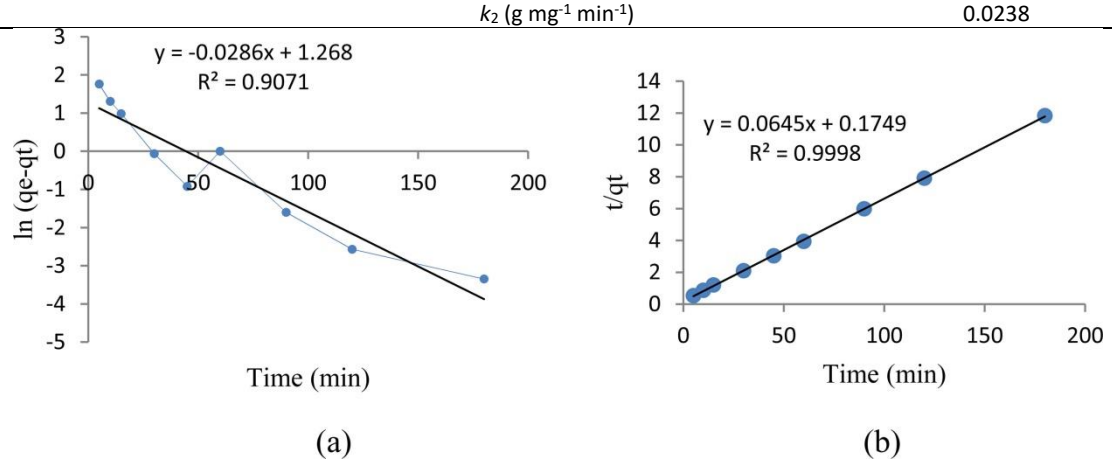

Figure 11. Graphs for (a) pseudo first-order, and (b) pseudo second-order

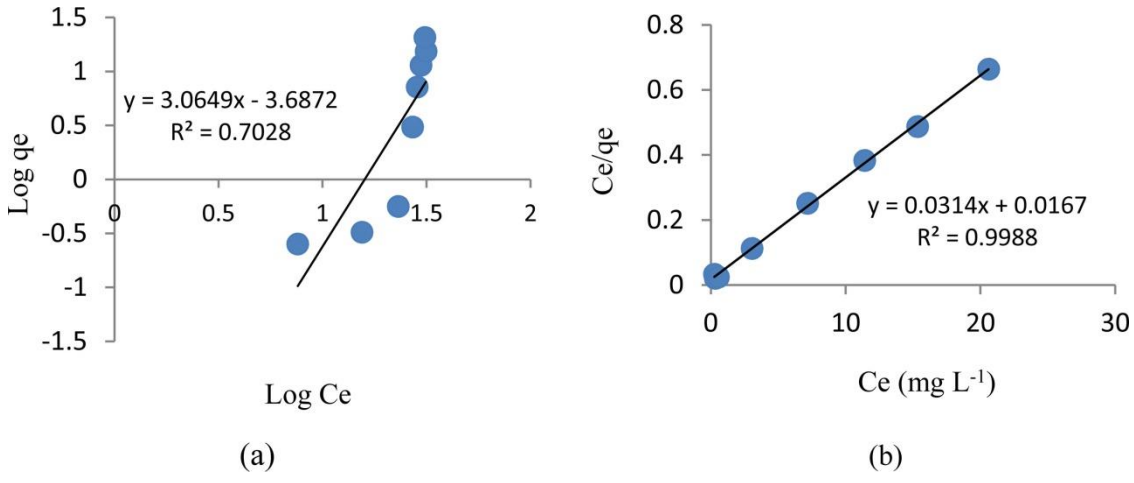

Figure 12. (a) Langmuir and (b) Freundlich plots for MB adsorption on zeolite/Fe_3O_4

Table 3. Isotherm adsorption parameters

Adsorption Isotherm	Parameter	Value
Freundlich model	K_F (mg g^{-1})	2.168 x 10^{-4}
	n	0.329
	R^2	0.7108
Langmuir model	q_m (mg g^{-1})	32.258
	K_L (L mg^{-1})	1.867
	R^2	0.999

3.2.6. Adsorption isotherm of MB by zeolite/Fe_3O_4

The adsorption capacity and other parameters were evaluated using Langmuir and Freundlich models. The equation for Langmuir and Freundlich isotherms are presented as Eq. 5 and Eq.6 respectively:

$$\frac{C_e}{q_e} = \frac{1}{q_m} C_e + \frac{1}{K_L \cdot q_m} \quad (5)$$

$$\log q_e = \log K_F + \frac{1}{n} \log C_e \quad (6)$$

Where q_e is the adsorption capacity, K_L is the adsorption constant.

The adsorption of MB from solution by zeolite/$Fe_3O_{4(33.30\%)}$ was fitted to both the Langmuir and Freundlich adsorption isotherm models as shown in Figure 12 and Table 3. The data in the table indicates that the Langmuir gives a better fit compared to the Freundlich adsorption isotherm. Accordingly, the model is best used to describe the single-layer adsorption processes. It is supposed that MB adsorption takes place in the homogeneous sites on the zeolite/Fe_3O_4 adsorbent. In contrast, the Freundlich isotherm is based on multi-layer, non-uniform, and heterogeneous adsorption of the adsorbate onto the adsorbent (Mouni *et al.*, 2017; Yuan *et al.*, 2018). The maximum adsorption capacity toward MB is found to be 32.258 mg g^{-1}. This capacity is higher than the capacity of unmagnetized Indonesian natural zeolite as reported by Saputra *et al.* (2019), that was as much as 14.94 mg g^{-1}. However the capacity is still lower compared to that of Fe_3O_4/clay for MB adsorption, that was 97 mg g^{-1} (Ge *et al.*, 2019) and that of Fe_3O_4/zeolite for Pb(II) adsorption that was 84 mg g^{-1} (Yuan *et al.*, 2018). An effort to improve the capacity of the Fe_3O_4/natural zeolite may be by attaching materials, such as chitosan (Kang *et al.*, 2018) or biochar (Meili *et al.*, 2019) that can extent its active surface area.

4. Conclusion

Recoverable zeolite/Fe_3O_4 adsorbents have been successfully produced by magnetization of the Indonesian natural zeolite having mordernite type with Fe_3O_4. The fraction of Fe_3O_4 in the adsorbent showed proportional effect on the adsorption capacity but gave opposite effect to the separable ability. A compromisingly good adsorption activity and separable ability was exhibited by zeolite/Fe_3O_4 with 33.30% of Fe_3O_4. The highest MB dye adsorption was reached by using 1.25 g L^{-1} of the adsorbent dose, pH 8, and 60 min. of the contact time. The adsorption kinetic well matched with pseudo second order and the adsorption rate was found as 0.0238 mg g^{-1} min^{-1}. The Langmuir isotherm best fitted to the MB dye adsorption, with the adsorption capacity of 32.258 mg g^{-1}.

Acknowledgment

The authors greatly acknowledge the financial support from Universitas Gadjah Mada through RTA Project No. 3194/UN1/DITLIT/DIT-LIT/LT/2019, April 11 2019.

References

Ahmed M.A., Abou-Gamra Z.M. and Salem A.M. (2017), Photocatalytic degradation of methylene blue dye over novel spherical mesoporous Cr_2O_3/TiO_2 nanoparticles prepared by sol-gel using octadecylamine template. *Journal of Environmental Chemical Engineering*, **5**(5), 4251–4261. https://doi.org/10.1016/j.jece.2017.08.014.

Altintig E., Altundag H., Tuzen M. and Sarı A. (2017), Effective removal of methylene blue from aqueous solutions using magnetic loaded activated carbon as novel adsorbent. *Chemical Engineering Research and Design*, **122**, 151–163. https://doi.org/10.1016/j.cherd.2017.03.035.

del Cotto-Maldonado M., Duconge O., Morant C. and Márquez F. (2017). Fenton process for the degradation of methylene blue using different nanostructured catalysts. *American Journal of Engineering and Applied Sciences*, **10** (2), 373–381. https://doi.org/10.3844/ajeassp.2017.373.381.

Eslami H., Khavidak S.S., Salehi F., Khosravi R., Fallahzadeh R., Peirovi R. and Sadeghi S. (2017), Biodegradation of methylene blue from aqueous solution by bacteria isolated from contaminated soil. *Journal of Advances in Environmental Health Research*, **5**, 10–15.

Fan S., Wang Y., Wang Z., Tang J. and Li X. (2017), Removal of methylene blue from aqueous solution by sewage sludge-derived biochar: Adsorption kinetics, equilibrium, thermodynamics and mechanism. *Journal of Environmental Chemical Engineering*, **5**(1), 601–611. https://doi.org/10.1016/j.jece.2016.12.019.

Ge M., Xi Z., Zhu C., Liang G., Hu G., Jamal L. and Alam J.S.M. (2019), Preparation and characterization of magadiite–magnetite nanocomposite with its sorption performance analyses on removal of methylene blue from aqueous solutions. Polymers, **11**, 607–622. https://doi.org/10.3390/polym11040607.

Javanbakht V., Ghoreishi S.M., Habibi N. and Javanbakht M. (2017), Synthesis of zeolite/magnetite nanocomposite and a fast experimental determination of its specific surface area. *Protection of Metals and Physical Chemistry of Surfaces*, **53**, 693–702. https://doi.org/10.1134/S2070205117040086.

Kang S., Zhao Y., Wang W., Zhang T., Chen T., Yi H., Rao F. and Song S. (2018), Removal of methylene blue from water with montmorillonite nanosheets/chitosan hydrogels as adsorbent. *Applied Clay Science*, **448**, 203–211. https://doi.org/10.1016/j.apsusc.2018.04.037.

Khodadadi M., Malekpour A. and Ansaritabar M. (2017), Removal of Pb (II) and Cu (II) from aqueous solutions by NaA zeolite coated magnetic nanoparticles and optimization of method using experimental design. *Microporous and Mesoporous Materials,* **248**, 256–265. https://doi.org/10.1016/j.micromeso.2017.04.032.

Meili L., Lins , P.V., Zanta C.L.P.S., Soletti J.I., Ribeiro L.M.O., Dornelas C.B., Silva T.L. and Vieira M.G.A. (2019), MgAl-LDH/Biochar composites for methylene blue removal by adsorption. *Applied Clay Science,* **168**, 11–20. https://doi.org/10.1016/j.clay.2018.10.012.

Mohseni-Bandpi A., Al-Musawi T.J., Ghahramani E., Zarrabi Z., Mohebi S. and Vahe S.A. (2016), Improvement of zeolite adsorption capacity for cephalexin by coating with magnetic Fe_3O_4 nanoparticles. *Journal of Molecular Liquids*, **218**, 615–624.

Mouni L., Belkhiri L., Bollinger J.C., Bouzaza A., Assadi A., Tirri A., Dahmoune F., Madani K. and Remini H. (2018), Removal of methylene blue from aqueous solutions by adsorption on Kaolin: Kinetic and equilibrium studies. *Applied Clay Science*, **153**, 38–45. https://doi.org/10.1016/j.clay.2017.11.034.

Pathania D, Sharma S and Singh P. (2017), Removal of methylene blue by adsorption onto activated carbon developed from *Ficus carica* bast. *Arabian Journal of Chemistry*, **10**(1), S1445–S1451. https://doi.org/10.1016/j.arabjc.2013.04.021.

Reza K.M., Kurny A. and Gulshan F. (2016), Photocatalytic degradation of methylene blue by magnetite+H_2O_2+UV process. *International Journal of Environmental Science and Development*, **7**(5), 325–329. https://doi.org/10.7763/IJESD.2016.V7.793.

Saputra A., Prameswari M.D., Kinanti V.T.D., Mayasari O.D., Sutarni Y.D., Apriany K. and Lestari W.W. (2017), Preparation, characterization and methylene blue dye adsorption ability of acid activated-natural zeolite. *IOP Conference Series: Materials Science and Engineering*, **172**, 012039. https://iopscience.iop.org/journal/1757-899X.

Somsesta N., Sricharoenchaikul V. and Aht-Ong D. (2020), Adsorption removal of methylene blue onto activated carbon/cellulose biocomposite films: Equilibrium and kinetic studies. *Materials Chemistry and Physics*, **240**, 122221. https://doi.org/10.1016/j.matchemphys.2019.122221.

Wong K.T., Eu N.C., Ibrahim S., Kim H., Yoon Y., *et al.* (2016), Recyclable magnetite-loaded palm shell-waste based activated carbon for the effective removal of methylene blue from aqueous solution. *Journal of Cleaner Production*, **115**, 337–342.

Yuan M., Xie T., Yan., G., Chen Q. and Wang L. (2018), Effective removal of Pb^{2+} from aqueous solutions by magnetically modified zeolite. *Powder Technology*, **332**, 234–241. https://doi.org/10.1016/j.powtec.2018.03.043.